

Optoelectronic Isolator for Microwave Applications

DAVID B. HUFF, MEMBER, IEEE, AND JOHN P. ANTHES

Abstract — A new family of devices is described. The microwave characteristics of high-speed semiconductor laser diodes and photodiodes allow the design of low-loss isolators at high frequencies. A prototype optoelectronic isolator has achieved, for the first time, forward transmission gain without the need for auxiliary amplification. The unilateral transformation between electrical and optical regimes has produced a device with high isolation (> 80 dB) and 0.13 dB gain. Prototype characteristics are compared to analytic models.

I. INTRODUCTION

ISOLATORS are used in microwave systems for two purposes: 1) to provide a defined impedance and 2) to prevent reverse-traveling signals from degrading system performance. Microwave receivers, for instance, use isolators at their input to provide fixed impedances to the input stages while some precision oscillators use isolators to prevent frequency pulling by external signals. For applications that require high isolation at RF frequencies, optoisolators using light-emitting diodes are used [3]. This paper describes an alternative optoelectronic isolator based upon semiconductor laser diode technology. This technology is suitable for use at microwave frequencies.

The development of semiconductor laser diodes capable of modulation at microwave frequencies has resulted in investigations of these devices as microwave isolators [1], [2]. Since a reverse-biased photodiode detector cannot emit light, a device using an optically coupled laser diode and photodiode is essentially unilateral; i.e., the component pair will only transmit signals in one direction. By reactive impedance matching both components over a limited bandwidth, and appropriate biasing, the change in impedance through the device can be used to provide forward power gain. The resultant circuit and its performance are analogous to a common-base RF transistor [4] without feedback capacitance or conductance.

This paper will describe the analysis, design, and implementation of a hybrid optoelectronic isolator for microwave applications. The device was designed to operate over a 300 MHz bandwidth centered at 3 GHz. The prototype achieved isolation greater than 80 dB and a

Manuscript received July 28, 1989; revised November 5, 1989. This work was supported by the U.S. Department of Energy under Contract DE-AC04-76DP00789.

D. B. Huff is with the Ortel Corporation, 2015 W. Chestnut St., Alhambra, CA 91803.

J. P. Anthes is with Sandia National Laboratories, Albuquerque, NM 87185.

IEEE Log Number 8934039.

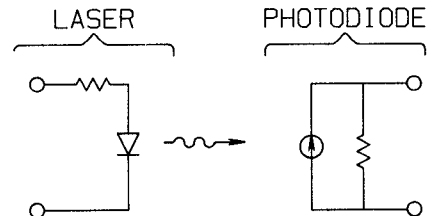


Fig. 1. Simplistic model of optoelectronic isolator.

forward power gain of 0.13 dB at its center frequency. Analytic results suggest that improved performance is possible.

II. DESIGN ANALYSIS

A. Ideal Characteristics

An ideal optoelectronic isolator using a high-speed semiconductor laser diode [5] and a high-speed photodiode [6] can be modeled as in Fig. 1. The laser diode is represented as a $5\ \Omega$ resistor, and the photodiode as a light-dependent current source shunted by a high resistance. Ideal laser diodes and photodiodes have quantum efficiencies of 100% so that, combined with a loss-free lens or optical waveguide, a current transfer ratio of 1:1 is possible. Furthermore, because laser diodes are low-impedance structures and photodiodes exhibit high impedance, microwave gain over some bandwidths can be realized by lossless reactive impedance matching of the diodes to the nominal system value (usually $50\ \Omega$). The gain that may be realized is dependent on the laser-diode-to-photodiode impedance ratio.

Optical signals, because of their short wavelength, can effectively propagate through apertures that are highly attenuating to microwaves. An optoelectronic isolator is truly unilateral if counterpropagating RF energy can be efficiently blocked. To ensure optoelectronic component isolation, the laser diode and the photodiode are first sealed in adjacent Faraday enclosures. Secondly, the laser diode light is efficiently transferred by a glass lens whose dimensions are selected to act as a cylindrical waveguide below cutoff to counterpropagating RF energy. It is important to ensure that the photodiode does not become forward biased during operation as it can emit light similar to an LED, and potentially disturb laser diode performance.

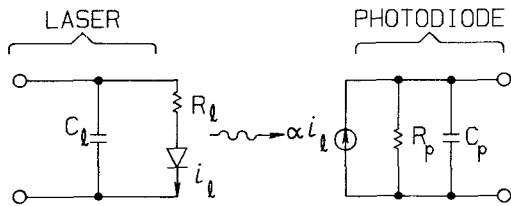


Fig. 2. Model of laser diode and photodiode showing parasitic capacitances C_l and C_p .

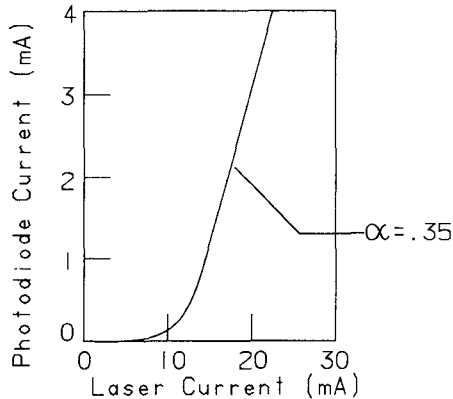


Fig. 3 The dc transfer efficiency of the optoelectronic isolator was 0.35 mA/mA.

B. Practical Implementation

Fig. 2 shows a more complete electrical model for the optoelectronic isolator. In this model, the laser diode impedance is represented by the parallel combination of resistance, R_l , and capacitance, C_l . The laser diode parasitic resistance is lumped into R_l . Wire-bond inductances are omitted here for simplicity. The current transfer ratio, α , is the product of the quantum efficiencies:

$$\alpha = \eta_l \cdot \eta_c \cdot \eta_p \quad (1)$$

of the laser diode, η_l , the photodiode, η_p , and the lens coupling efficiency, η_c . The photodiode impedance is represented by the parallel combination of resistance, R_p , and capacitance, C_p .

The dc transfer curve for an optoelectronic isolator is shown in Fig. 3. It shows a flat portion below the lasing threshold current and a linear sloped portion above the lasing threshold. Microwave modulation of the light intensity of the laser occurs by varying the current into the laser about some dc bias level above the threshold current. In this context, the value for η_l is determined by the differential (slope) efficiency of the laser at the bias current. Additionally, the light intensity modulation depth follows a second-order, low-pass profile (see Fig. 4). Below the cutoff frequency, termed the laser resonance frequency, F_r , the response is essentially flat with some peaking near the resonance frequency. Above resonance, the response rolls off at 12 dB per octave. The resonance frequency is directly related to the laser internal power, P_0 , by [5]

$$F_r = \frac{1}{2\pi} \sqrt{\frac{A \cdot P_0}{\tau_p}} \quad (2)$$

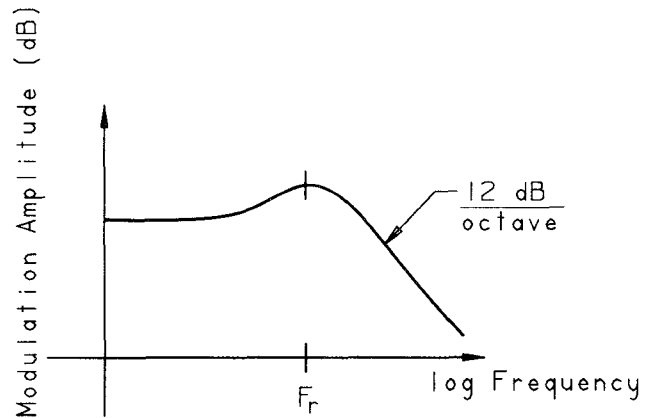


Fig. 4 Typical frequency response of semiconductor laser diode at one particular dc bias level.

where A is a constant and τ_p is the photon lifetime in the laser cavity. These parameters depend on laser construction while power, P_0 , is linearly dependent on injection current, so that

$$F_r \propto \sqrt{i - i_{th}} \quad (3)$$

where i is the total current in the laser diode and i_{th} is the laser threshold current.

C. Analysis

Power gain can be achieved with a circuit over a limited bandwidth due to the impedance transformation from R_l to R_p .

Representing the impedance matrix of the isolator as

$$Z = \begin{pmatrix} Z_{11} & Z_{12} \\ Z_{21} & Z_{22} \end{pmatrix} \quad (4)$$

then, by inspection of Fig. 2,

$$Z_{11} = Z_{in} = \frac{1}{j\omega C_l} \parallel R_l \quad (5a)$$

$$Z_{22} = Z_{out} = \frac{1}{j\omega C_p} \parallel R_p \quad (5b)$$

$$Z_{21} = \alpha \cdot \frac{1}{j\omega C_p} \parallel R_p \cdot \frac{1}{1 + j\omega R_l C_l} \quad (5c)$$

and, since the device is unilateral,

$$Z_{12} = 0. \quad (5d)$$

Converting to S parameters using the identities [7]

$$S_{21} = \frac{2 \cdot Z'_{21}}{(Z'_{11} + 1)(Z'_{22} + 1)} \quad (6a)$$

$$S_{ii} = \frac{Z'_{ii} - 1}{Z'_{ii} + 1} \quad \text{for } i = 1, 2 \quad (6b)$$

where the primed notation indicates normalization to the system impedance, Z_0 (usually 50 Ω) and assuming ideal

impedance matching, the maximum unilateral gain [8], $G_{u,\max}$, is

$$G_{u,\max} = |S_{21}|^2 \cdot \frac{1}{1 - |S_{11}|^2} \cdot \frac{1}{1 - |S_{22}|^2} \quad (7a)$$

which, on substitution, gives

$$G_{u,\max} = \frac{4\alpha^2 R_p^2}{[(R_I + 1)^2 - (R_I - 1)^2][(R_p + 1)^2 - (R_p - 1)^2]} \quad (7b)$$

which simplifies to

$$G_{u,\max} = \left[\frac{\alpha^2}{4} \right] \cdot \left[\frac{R_p}{R_I} \right] \quad (8)$$

for an ideal impedance match at a given frequency. Thus the ideal impedance matched gain that can be achieved is dependent only on α^2 and the ratio R_p/R_I . Interestingly, this result is independent of the diode's capacitances and Z_0 , the system impedance value.

D. Isolation

Determination of the electromagnetic coupling through a small aperture in a common conducting planar wall between regions has previously been studied [9]–[11]. The isolation of the optoelectronic isolator is dependent upon its mechanical structure and on the frequency spectrum contained in reverse-traveling signals. Leakage signals can propagate between the chambers if poor construction methods are used. Assuming the laser diode and photodiode are in ideal Faraday enclosures, reverse coupling between them depends upon the dimensions of the connecting aperture containing the lens, the frequency of the signal, and the dielectric constant of the lens. Resonance microwave coupling associated with the characteristic dimensions [2] of the Faraday enclosures may also have to be considered.

Extremely high attenuation of counterpropagating signals is obtained when the lens dimensions are selected to be much smaller than the cutoff wavelength of a dielectric-filled cylindrical waveguide. The effective dimensions of the aperture are increased by the dielectric material used in the lens. For fused silica ($\epsilon_r = 3.78$), the transmission is increased by a factor of 54 compared to the air-filled case. In general, calculations [11] show the isolation increases as the frequency is lowered, the length is increased, or the diameter of the aperture is decreased. Small changes in dimensions can strongly affect microwave leakage.

III. IMPLEMENTATION

A. Device Characteristics

The laser diode used was a GaAlAs buried heterostructure design operating at 810 nm. The back facet was coated for > 90% reflectivity. The optical power versus injection current is shown in Fig. 5 and shows a 0.63 W/A differential slope efficiency above threshold (which corresponds to 41% quantum efficiency). Similarly, the photodiode

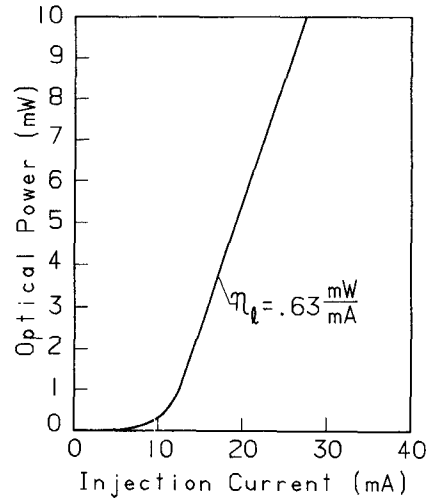


Fig. 5. Laser diode light intensity as a function of injection current. Slope efficiency of this laser was 0.63 mW/mA.

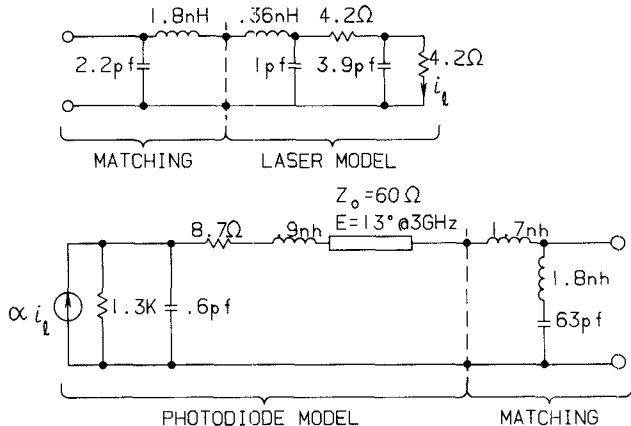


Fig. 6. Final electrical models used for laser diode, photodiode, and for complementary matching circuits.

ode was a GaAlAs p-i-n photodiode that was antireflection coated. The photodiode responsivity at 810 nm was 0.61 A/W (95% quantum efficiency). Ideal loss-free optical coupling would result in a $0.63 \cdot 0.61 = 0.386$ A/A current transfer ratio. Accounting for the 10% optical coupling loss ($\eta_c \approx 0.9$) in our prototype isolator, the actual dc current transfer ratio, α , was 0.347 A/A, corresponding to a loss of $20 \log(0.347) = -9.2$ dB.

Microwave characteristics for the laser diode and photodiode were measured with a network analyzer to determine their equivalent circuits. The models used are shown in Fig. 6 along with calculated values. These models also account for frequency-dependent parasitic losses, which can reduce isolator efficiency at microwave frequencies. In addition, in the prototype isolator, the laser bias current was adjusted for coincidence of the laser resonance with the operating frequency. This maximized forward transmission of the isolator.

B. Isolator Construction

The laser diode and the photodiode with their respective matching circuits were mounted in separate compartments

of a two-piece housing. The laser compartment was RF tight with the exception of the requisite 2.0 mm diameter lens mounting hole. A high numerical aperture ($NA = 0.6$) GRAded INdex (GRIN) lens was mounted in this hole. Silver epoxy was used on the lens/housing interface to ensure Faraday integrity. Optical coupling was accomplished with the lens parameters selected to collect all available light and produce a focused laser spot. The spot size was matched to the photodiode 50- μ m-diameter active area. For practical considerations, measurement of forward transmission was performed with active alignment of the two-piece housing.

Measurement of the reverse transmission characteristics was performed with the housings mated together. In order to verify that there was no resonant coupling between the housings that could move near the 3 GHz center frequency with changes in construction, the reverse isolation was measured from 45 MHz to 20 GHz. No leakage was observed.

Because reflected laser light returning to the laser active area can disturb the laser's performance, precautions were taken to prevent retroreflections. First, all components were antireflection coated. Also, the photodiode was angled away from normal incidence. Lastly, component spacing was chosen to place all reflection-induced disturbances well outside the operating bandwidth of the device. Specifically, reflection round-trip time was ~ 25 ps, corresponding to disturbances at about 40 GHz. No reflection-induced disturbances were observed.

Matching circuits were designed using the model presented in Fig. 6. They were simple two-element networks designed to minimize loss at center frequency. No attempt was made to maximize bandwidth or reduce sensitivity to differences in optoelectronic components. Inductors in the matching circuits were realized with bond wires; the capacitors were of a single-layer chip design.

The laser diode circuitry did not require tuning, while the photodiode circuit, due to the higher sensitivity of the design, did require tuning. This was accomplished by moving the bond-wire locations and adjusting the photodiode bias, which changed its junction capacitance. The housings were designed to hold microwave integrated circuits (MIC's) so that different designs and operating frequencies could easily be tried.

C. Results

Several different GRIN rod lenses, with variations in the NA and diameter, were tried. Best results were obtained with a 0.22 pitch, 1.8-mm-diameter, 0.60 NA plano-convex GRIN lens with antireflection optical coatings from NSG America.

Operating levels were set to produce optimized performance of the prototype optoelectronic isolator. The laser diode dc bias level was 12.9 mA, which moved the laser resonance to 3 GHz. The photodiode bias voltage was 19 V. The useful portion of the laser diode injection

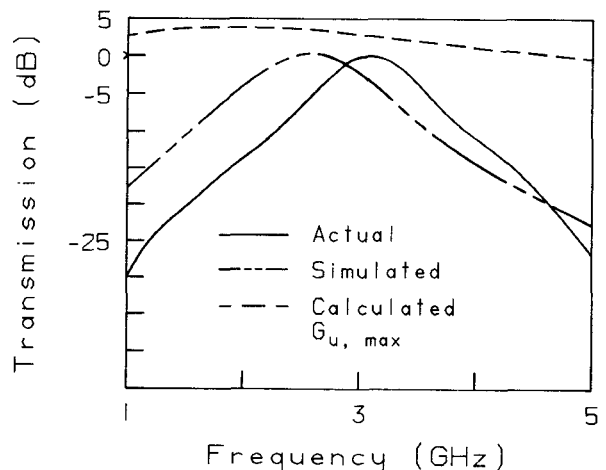


Fig. 7 Forward transmission response (S_{21}) of the isolator. Also shown are computer simulations of the forward transmission and maximum available gain ($G_{u,\max}$)

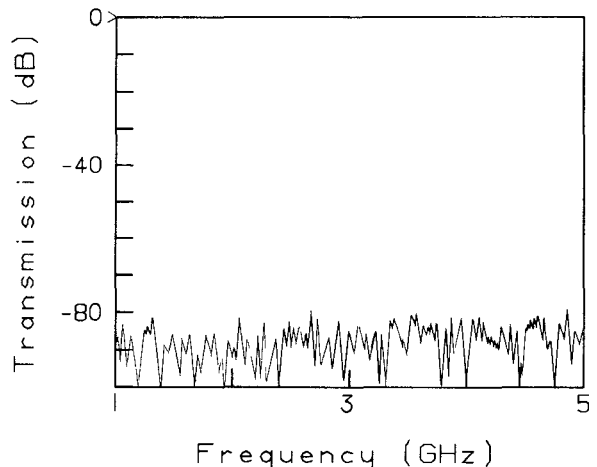


Fig. 8 Reverse transmission response (S_{12}) of the isolator.

current above the lasing threshold was 2.5 mA. The resulting photocurrent was 880 μ A when the photodiode was aligned to maximize forward transmission.

Fig. 7 shows the forward transmission response in the 1–5 GHz frequency range. The best transmission results after tuning were 0.13 dB gain centered at 3.2 GHz with a 850 MHz 3 dB bandwidth. Numerical simulations¹ of the isolator forward transmission, $|S_{21}|$, and $G_{u,\max}$ based on the model in Fig. 6 are also included. The measured and simulated results show quite good agreement with the shift in center frequency, probably due to inaccuracies in the parasitic element values and circuit tuning. Fig. 8 shows the reverse transmission characteristics. For this measurement, the housings were mated with a common cover. The measured reverse transmission, $|S_{12}|$, was less than -80

¹Numerical simulations were performed using Touchstone(R), Version 1.6, March 1988, from EEsol, Inc., 6795 Lindero Canyon Road, Westlake Village, CA 91362.

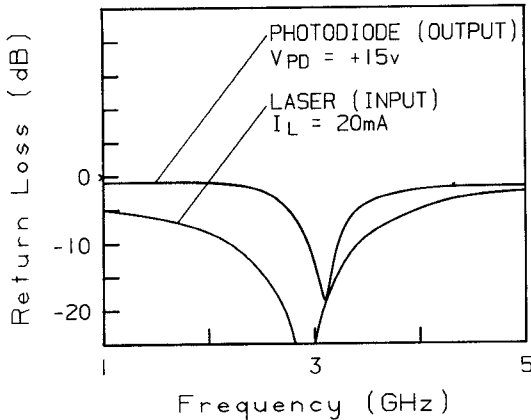


Fig. 9. Return loss at laser input (S_{11}) is the bottom curve and return loss at photodiode output (S_{22}) is the top curve.

dB (the system measurement limit) over the 1–5 GHz frequency band.

Fig. 9 shows the return losses for both the laser diode and the photodiode modules. High return loss, corresponding to low reflected microwave power, is a measure of the quality of the impedance match to the devices. For the laser, this was greater than 10 dB over the 3 dB bandwidth of the isolator. The photodiode circuit, because of the higher impedance ratio needed to match the device, exhibited more narrow-band performance. As a result, the photodiode return loss was greater than 6 dB, with a peak value greater than 15 dB at center frequency.

For dc operation, we measured a 9.2 dB insertion loss. The laser diode and the photodiode added an additional 2 dB of parasitic losses at the 3 GHz center frequency. Therefore, more than 11 dB was gained by the impedance matching circuitry. Using expression (8) with resistance values shown in the Fig. 6 circuit model, the analytical prediction of maximum transmission was

$$G_{u,\max} = 6.6 \text{ dB.}$$

Accounting for the 2–3 dB of additional gain due to the coincidence of the laser diode resonance peak with the isolator center frequency, the total predicted gain was ~9 dB. If the contact resistance in the model is reduced to 0.2 Ω , the simulated $G_{u,\max}$ is 5.3 dB, which compares well with the analytically obtained 6.6 dB.

IV. CONCLUSIONS

We have constructed a prototype optoelectronic isolator that achieved, for the first time, unamplified power gain of 0.13 dB at 3 GHz. This result contrasts strongly with a 26 dB insertion loss reported previously [2].

We have also developed a simple analytical model showing that the unamplified “gain” that can be achieved is dependent only on α^2 and the impedance ratio R_p/R_l . Analytical models indicate that an ideal optoelectronic

isolator can exhibit up to ~9 dB power gain. Measured results, analytic calculations, and numerical simulations were consistent. Further development efforts with optimized laser diodes, photodiodes, and optical coupling techniques are required to approach these predicted performance levels.

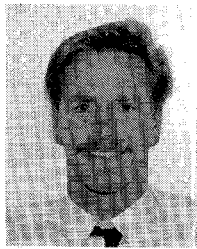
Within the scope of practical device implementation, a new family of devices incorporating the microwave properties of high-speed optoelectronic components has been demonstrated. Prototype results indicate that use of this device in an operating system can control self-oscillation in high-gain receivers and/or provide useful isolation of sensitive radars. Furthermore, the required size is smaller, especially with monolithic implementation, while providing isolation far in excess of competing technologies. For comparison, a packaged ferrite isolator would be about twice the size of the prototype while providing only 30 dB of isolation.

ACKNOWLEDGMENT

The authors are pleased to acknowledge helpful discussions with Dr. I. Ury at Ortel Corporation, Alhambra, CA, and with R. O’Nan and R. Knudsen, both at Sandia National Laboratories, Albuquerque, NM. R. Knudsen also performed the numerical simulation in subsection III-C. The authors also wish to recognize the encouragement offered by Dr. D. B. Hayes at Sandia National Laboratories.

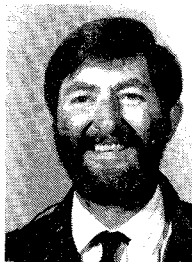
REFERENCES

- [1] R. A. Kiehl and D. M. Drury, “Performance of optically coupled microwave switching devices,” *IEEE Trans. Microwave Theory Tech.*, vol. MTT-29, pp. 1004–1010, 1981.
- [2] J. P. Anthes, P. Garcia, K. Y. Lau, and I. Ury, “High speed optical isolator for radar applications,” in *Picosecond Electronics and Optoelectronics*, by F. J. Leonberger, C. G. Lee, F. Capasso, and H. Morkoc, Eds. (Springer-Verlag Series in Electronics and Photonics, vol. 24). Berlin, Heidelberg, New York, and Tokyo; Springer-Verlag, 1987, pp. 285–288.
- [3] A. Helfrick, “An optically coupled VCO,” *RF Design*, pp. 29–30, July 1988.
- [4] R. H. Rediker, T. N. Quist, and B. Lax, “High speed heterostructure photodiodes and beam-of-light transistors,” *Proc. IEEE*, vol. 51, pp. 218–219, 1963.
- [5] K. Y. Lau and A. Yariv, “Ultra-high speed semiconductor lasers,” *IEEE J. Quantum Electron.*, vol. QE-21, no. 2, pp. 121–138, 1985.
- [6] N. Bar-Chaim, K. Y. Lau, I. Ury, and A. Yariv, “High-speed GaAlAs/GaAs PIN photodiode on a semi-insulating substrate,” *Appl. Phys. Lett.*, vol. 43, no. 3, pp. 261–262, 1983.
- [7] R. W. Anderson, “S-parameter techniques for faster, more accurate network design,” *Hewlett-Packard J.*, vol. 18, no. 6, pp. 1–12, 1967.
- [8] T. T. Ha, *Solid State Microwave Amplifier Design*. New York: Wiley, 1981, p. 35.
- [9] H. A. Bethe, “Theory of diffraction by small holes,” *Phys. Rev.*, vol. 66, nos. 7–8, pp. 163–182, 1944.
- [10] N. A. McDonald, “Electric and magnetic coupling through small apertures in shield walls of any thickness,” *IEEE Trans. Microwave Theory Tech.*, vol. MTT-20, pp. 689–695, 1972.
- [11] J. P. Anthes, “Analytical design of a high bandwidth optoelectronic signal link for use in an EMP pulse radiation environment,” in *Proc. IEEE ISE Symp. (Albuquerque, NM)*, May 10–12, 1988, pp. 109–115.



David B. Huff (M'87) received the B.S.E.E. degree from the California Institute of Technology, Pasadena, in 1983.

From 1983 to 1986 he worked as a microwave design engineer at Hughes Aircraft Co., Space and Communications Group. In 1986, he joined the Ortel Corporation, where he is currently Manager of Microwave Product Development.



John P. Anthes received the B.S. degree from California State University, Fullerton, in 1972 and the M.S. degree from the University

of Southern California in 1974. Both degrees, in physics, emphasized solid state laser physics.

He is a Senior Member of Technical Staff at Sandia National Laboratories. During the last five years, his work has been directed toward military applications of optoelectronic components. Previously, his research focused on inertial confinement fusion experiments using high-energy laser systems or using high-energy, pulsed-power accelerators. Through his involvement in research and development at Sandia, he has published over 75 papers in these subject areas.

Mr. Anthes is a member of the Optical Society of America and a member of the Laser Sciences and the Plasma Physics Divisions of the American Physical Society.